Surrogate models to unlock the optimal design of stiffened panels accounting for ultimate strength reduction due to welding residual stress

Coraddu, Andrea; Oneto, Luca; Li, Shen; Kalikatzarakis, Miltiadis; Karpenko, Olena

DOI
10.1016/j.engstruct.2023.116645

Publication date
2023

Document Version
Final published version

Published in
Engineering Structures

Engineering Structures 293 (2023) 116645

Contents lists available at ScienceDirect

Engineering Structures

journal homepage: www.elsevier.com/locate/engstruct

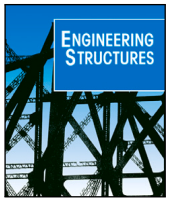

Surrogate models to unlock the optimal design of stiffened panels accounting for ultimate strength reduction due to welding residual stress

Andrea Coraddu [a,*], Luca Oneto [b], Shen Li [c], Miltiadis Kalikatzarakis [c], Olena Karpenko [a]

[a] Delft University of Technology, Delft, The Netherlands
[b] University of Genoa, Genova, Italy
[c] University of Strathclyde, Glasgow, United Kingdom

ARTICLE INFO

Keywords:
Stiffened panels
Optimal design
Ultimate strength reduction
Welding residual stress
Nonlinear finite element methods
Surrogate models

ABSTRACT

In this paper, for the first time, a three-step approach for the optimal design of stiffened panels accounting for the ultimate limit state due to welding residual stress is developed. First, authors rely on state-of-the-art analytical approaches coupled with recently data-driven nonlinear finite element methods surrogates characterized by functional which are computationally expensive to build but computationally inexpensive to use. Then, surrogates are used within a design optimization loop to find new optimal designs since nonlinear finite element methods are too computationally demanding for this purpose. Finally, the new designs are reassessed with the original nonlinear finite element methods to verify that substituting them with their surrogates in the optimization loop actually leads to better designs. Results obtained optimizing a series of parameters of a commonly used stiffened panel geometry under different scenarios will support the authors' novel approach.

1. Introduction

The structural design of large-scale engineering infrastructures, such as ships, offshore floaters, bridges, and aircraft, would typically experience a process of prototype, appraisal, and optimization [1]. The prototype of engineering structures usually relies on several existing designs with similar operational profile [2]. The variations are made taking into account of the changes in, e.g., operational demand, budget, construction capability, and owner's request. Finally, the appraisal of a prototype structural design is performed by limit state assessment, which is a proven design philosophy and has been widely adopted across different disciplines in recent years [3]. Four limit states are relevant for structural design, namely Serviceability Limit State, Fatigue Limit State, Accidental Limit State, and Ultimate Limit State (ULS) [4–7]. Serviceability Limit State is determined by limiting values that are oriented toward the normally envisaged use of a structural system [8]. Fatigue Limit State refers to the failure due to cumulative damage of repeated loading that leads to the initiation and propagation of cracks and eventually fractures [9]. Accidental Limit State examines the damage tolerance of structural systems in an accidental event, such as collision, grounding, fire, and explosion [10]. ULS concerns the maximum load-carrying capacity of the structures and is a typical assessment criterion in the initial design, i.e., prototyping [11–13]. A rigorous limit state-based appraisal would ensure the safety of structural design [12]. In the present paper, ULS will be considered since it is the main criteria adopted in the initial design phase for determining the principal scantlings of structures [14,15].

The prototype design is normally an adaptation of the existing structure induced by engineering knowledge with limited support from automatic tools. This usually results in structural scantling that will not be optimized for the specific requirements [16], leading to overly conservative structural designs [17]. Instead, an optimal structural design would have various economical, technological, and environmental benefits [17]. For example, in the commercial sectors, an optimal structural design implies a significant saving on the initial investment and the life-cycle cost [18]. In the defense sector, the optimization of structures could enhance the structural integrity and damage tolerance while retaining a lightweight configuration, which is a crucial issue for weight-sensitive structures [19,20]. In terms of the environmental impact, optimizing the structural design may also improve the operational efficiency of an engineering system, which potentially reduces its life-cycle carbon footprint [21]. Structural optimization is therefore a fundamental issue to be addressed and there is a strong demand for effective and efficient supporting tools [22]. In fact, current optimization strategies mostly rely on engineering judgments and experience

* Corresponding author.
E-mail addresses: a.coraddu@tudelft.nl (A. Coraddu), luca.oneto@unige.it (L. Oneto), shen.li@strath.ac.uk (S. Li), miltiadis.Kalikatzarakis@strath.ac.uk (M. Kalikatzarakis), o.karpenko@tudelft.nl (O. Karpenko).

https://doi.org/10.1016/j.engstruct.2023.116645
Received 20 March 2023; Received in revised form 16 June 2023; Accepted 19 July 2023
Available online 3 August 2023

complemented with a series of trial-and-error procedures [23,24] which may not lead to the best structural design [25].

Within the ULS-based design, the structural assessment can be performed using analytical approaches, empirical formulations, and numerical methods [26]. Analytical approaches [27] are usually developed based on the classical structural stability theory, with appropriate consideration of the plasticity effect. The recommended approach in Common Structural Rule (CSR) is one of the typical analytical approaches [28]. Empirical formulations [29] in structural engineering are conventionally derived by simple curve fitting. Numerical methods [30] typically refer to finite element methods and, more often, Nonlinear Finite Element Methods (NLFEMs). NLFEM is considered to be the most accurate approach since it is able to consider all interacting buckling failure modes and the material yielding [31]. Moreover, NLFEM enables the analysts to account for different boundary conditions, imperfections and load combinations while analytical and empirical methods can be limited to specific configurations that may be difficult to extend [32]. For example, NLFEM allows incorporating the Welding-induced Residual Stress (WRS) in an ULS-based structural assessment [33], while addressing this with CSR formulations can be problematic [34]. Nevertheless, accounting for the WRS in the NLFEMs comes with a price: a minimum of two NLFEM simulations (i.e., with and without residual stress) are needed to quantify the effect of residual stress [35] and each NLFEM simulation takes minutes/hours [36]. If the number of structural designs to be assessed is small, this computational effort can be acceptable (i.e., when supporting the human structural design handcrafting). When NLFEMs are incorporated into an automatic optimization loop, the computational demand can be substantial, owing to the possibility of numerous iterations being required. This significant computational burden is a direct consequence of the iterative nature of optimization processes, imposes a significant challenge to the practicality of employing NLFEMs in these settings. Specifically, the computational burden may exceed the available resources, thereby precluding the application of these methods in real-world scenarios. The infeasibility of this application underscores the inherent limitations of current computational resources when dealing with complex, non-linear models [37]. This is the main reason why currently the prototype design is usually an adaptation of the existing structure induced by engineering knowledge.

In order to address this barrier, many simplified approaches have been developed to predict the ULS of stiffened panels which allows for an efficient assessment and integration with different structural optimization schemes [38]. CSR approach is a typical example and well recognized by both research community and industry. When the residual welding stress is not taken into account, CSR is surely an effective solution [28] that allows avoiding the computational burden of NLFEMs [34,39–41] and maintaining enough accuracy to perform preliminary design optimization [28]. Unfortunately, the same approach is not easily adaptable to take into account the effect of residual stress [34] because of the complexity of the relation between the strength reduction and structural configurations. For this purpose, in this work, authors will rely on data-driven surrogate models of the NLFEMs [42]. Data-driven methods (DDMs) [43,44], in fact, allow for accurately approximating the NLFEMs without requiring the design of grounded simplifications. DDMs are able to automatically learn a functional representation of the NLFEM using a series of data generated by running multiple times the NLFEM. The advantage of this approach is that the learned functional is computationally inexpensive to apply, addressing the limitations of the NLFEM. The disadvantage is that this function is computationally expensive to build. In fact, building a model using DDMs requires running NLFEMs code multiple times to generate the data and then training the functional with a Machine Learning (ML) algorithm. Nevertheless, once this procedure is completed, the resulting learned functional can be reused inexpensively as many times as necessary allowing its use in an optimization loop. As a consequence it is possible to switch from a knowledge based adaptation of existing structure to a fully automated optimization process.

In fact, once addressed the computational barrier with the use of surrogate models, authors will develop an optimization problem and an optimization framework able to automatically find the optimal structural design: a design able to simultaneously minimize the weight and maximize the strength of the panels. In order to solve the optimization problems, authors will employ different state-of-the-art optimization algorithms, namely, the Interior-Point (IP) [45], the Active-Set (AS) [46], the Genetic Algorithm (GA) [47], and the Particle Swarm Optimization (PSO) [48].

Finally, the designs discovered during the optimization step are reassessed with the original NLFEMs to verify that substituting the NLFEMs with their surrogates in the optimization loop actually leads to better designs.

Results obtained optimizing a series of parameters of a commonly used stiffened panel geometry under different scenarios will support authors' proposal. Authors considered the stiffened panel since it is one of the most common solutions for structural design [11,49–51]. Moreover, their manufacturing is usually completed through welding and as a result, initial imperfections are induced in the structures taking the form of geometric deflection and WRS [15]. As shown by comprehensive studies such as [19,40,52–55], the ULS of stiffened panels is strongly influenced by the initial imperfections induced by the welding.

The remainder of this paper is structured as follows. Section 2 will present the state-of-the-art literature on structural optimization and the use of surrogate models for optimization. Section 3.1 will provide a description of the specific problem that authors want to address in this paper. Section 3.2 will present the formalization of the optimization problem under consideration, how authors optimized it, and where the surrogates are employed to reduce the computational burden. Results obtained optimizing a series of parameters of a commonly used stiffened panel geometry under different scenarios are reported in Section 4. Section 5 concludes the paper.

2. Related works

Structural design optimization is the focus of many researchers and practitioners that faced the problem with many different approaches [56,57].

Recently a quite complete review paper on structural size optimization techniques has been published [58]. Nevertheless, it is worth mentioning some other recent interesting works that inspired authors research.

Authors of [59] propose to optimize the structural weight of truss frames using PSO subject to constraints on the stress and displacement of each bar element. Optimization of reinforced concrete structure with shear walls was presented in [60], where the construction cost was optimized and constrained by structural strength and displacement achieving a cost reduction of 16%.

Authors of [61] developed a structural model for the support structures of wind turbines optimizing the weight of the support structure and constraining the level of vibration, stress, deformations, buckling, and fatigue. GAs were adopted leading to a mass reduction of 19.8%.

A reliability-based design optimization was conducted in [62] for Folded Pendulum Tuned Mass Dampers installed in a tall building subjected to turbulent wind excitation. Uncertainties in the system parameters and the wind excitation were taken into account. A Kriging-based Efficient Global Optimization (EGO) scheme was employed to speed up the convergence of the global search for the minimum annual probability of failure, in which a failure probability reduction of 83% was reported.

The authors of [63] introduced a computationally efficient optimal design approach for suspension bridges. An enhanced particle

swarm optimization (EPSO) was employed using a particle categorization mechanism to handle the constraints instead of the commonly used penalty method to improve the computational efficiency of the optimization procedure.

Genetic algorithm-based optimization was presented in [64] for a floor system based on steel web core sandwich panels with polyurethane (PUR) foam core taking into consideration structural, thermal, and acoustic performance using design code formula. In addition to structural mass, the study also addressed the optimization cost and environmental impact.

The optimization of a 542 m three-span cable-stayed bridge was considered in [65]. A sequential quadratic programming method was adopted, and it was shown that a 40% reduction of the sum of construction and repair costs could be achieved.

A multi-scale design methodology for the deterministic least-weight optimization of thin-walled composite structures was discussed in [66], integrating a global–local approach for the assessment of the buckling strength and a dedicated strategy to recover blended stacking sequences.

A multi-objective optimization for the B-pillar and rocker subsystems of battery electric vehicles was presented by the authors of [67] optimizing the structural weight, construction cost, and the mean crushing force of the B-pillar and rocker.

A fourth-order response surface model was developed to surrogate the direct finite element simulation. Optimization using a multi-objective artificial tree algorithm was used to build the Pareto front. Structural optimization was performed by authors of [68] for a 20MW wind turbine blade: the structural weight has been optimized with a set of realistic design constrained to ensure structural feasibility and aero-elastic stability. A sequential gradient-based optimization method was adopted, and a 2.66% reduction of structural weight was achieved.

Authors of [69] proposed a multi-objective optimization framework for ship structures optimizing the weight and surface area for a high-speed vehicle–passenger catamaran; simple allowable stress principle-based calculation was performed for the structural strength evaluation to constraint the design process. GAs were employed to build the Pareto front. Similarly, structural weight optimization was performed in [70] where strength constraint was evaluated using allowable stress principle-based classification rules. Optimization on two trimarans using a multi-island GA gave a reduction of the structural weight of 32.85% and 8.95%, respectively. The previously mentioned works' limitations are that limit state design was not employed for strength and safety evaluation to constrain the design optimization process. In this context, seminal works on ULS-based structural design optimization appeared in the literature [16,71,72]. These studies present multi-objective optimization problems for ship structural design targeting both weight and safety. The ULS-based safety assessment was performed using the semi-analytical computer code ALPS/ULSAP for stiffened panels and ALPS/HULL for ship hull girders [73]. GA and PSO algorithms were adopted, by which weight reductions of 1.4% and 2.3% were achieved on ship hull girder models respectively.

Instead of focusing on ULS, other work focused on Accidental Limit State. For example, authors of [74] proposed an Accidental Limit State aware structural design optimization of the side shell structures of ships. A case study on a chemical tanker was investigated focusing on structural crashworthiness as an optimization objective without optimizing the weight. PSO algorithm was employed leading to a 500% increase in the energy absorption capability increasing the structural weight by 18%. Nevertheless, these works also have practical limitations, as they required a large number of high fidelity simulations (e.g., with NLFEMs) and this prevents their use due to prohibitive computational requirements. To address this problem, surrogate models have been employed. For instance, authors of [75] investigated the optimization of the shear wall layout of high-rise buildings, surrogating the computationally expensive assessment of total mass, story drift, and the period ratio of a candidate building, using Support Vector Machines and Tabu Search. The authors demonstrated the feasibility of their approach with a series of case studies, with the reported results showing that feasible designs with a weight reduction of approximately 24% could be generated regardless of the building layouts and the loading scenarios considered. Authors of [76] employed surrogates to optimize carbon-fiber-reinforced plastic and concrete-filled steel tube columns. Employing a dataset of 200 experiments, they rely on XGBoost and Adaboost to surrogate the computation of the ultimate torsion strength and insert it in a multi-objective optimization problem (solved with a GA) with the aim to simultaneously minimize the material construction cost and maximize the torsional strength of a tube column. The reported results demonstrated that the framework was capable of identifying low-cost and high-strength geometries, with material savings of up to 40%, and with the authors further underlying its computational efficiency and suitability during the early design stage.

Authors of [77] presented a surrogate-based optimization framework for curvilinearly stiffened panels for the aerospace industry. As FEM-based optimization methods for aircraft panels with arbitrary curvilinear stiffeners are computationally demanding they surrogate the estimation of the buckling response of the panels utilizing Deep Neural Networks trained using data generated from 50,000 simulations. Subsequently, they use this surrogate in the optimization process (solved with PSO) minimizing the panel weight. The feasibility of the proposed framework was demonstrated in two case studies showing weight reductions up to 20%, with savings in computational requirements. Another case study with curvilinear stiffened panels was conducted by the authors of [78]. An image-based structural layout was employed to characterize the curvilinear stiffeners surrogating (with Convolutional Neural Networks) the buckling load and weight of the panels, utilizing a dataset of 250 FEM simulations. Subsequently, an optimization problem (solved with GA) was formulated with the aim to minimize panel weight subject to buckling load requirements. Authors were able to achieve state-of-the-art results compared with respect to traditional FEM-based optimization, with a weight reduction of 25%, and significantly lower computational time requirements.

Another interesting approach was proposed by the authors of [79] who employed Q-learning and GAs for ship structural optimization, focusing on a bulk carrier. A multi-objective optimization framework was developed, aiming to minimize the weight of the midship section of the case study vessel and the cumulative fatigue damage of the joint part of the bottom longitudinal and transverse bulkhead, which is one of the key checking points of a contemporary bulk-carrier. Unlike the previous studies presented thus far, a DDM was employed, not to approximate the output of a computationally expensive fatigue assessment but to guide the GA towards the generation of suitable candidates during the optimization procedure. Promising results were reported, with the proposed approach being able to consistently provide designs of reduced weight by up to 10% for the same fatigue damage.

A machine learning-based framework for optimal seismic design of structures was developed by authors of [80]. Multi-objective design optimization of a braced framework was investigated. The inter-story drift ratio parameter was predicted in a computationally efficient manner through the use of different DDMs.

Design optimization was reported for a compressive yielding beam in [81], where a multi-objective optimization was considered to maximize two competing performance indices, namely moment capacity and ductility. An integrated model was proposed based on different DDMs for the design performance evaluation. The GA-based optimization showed that improved moment capacity (84% increment) or ductility (75% increment) could be achieved for the compression-yielding beam with a rectangular section compared with the initial reference design.

3. Methodology

In this paper, for the first time, a three-step approach for the optimal design of stiffened panels accounting for the ultimate limit state due to

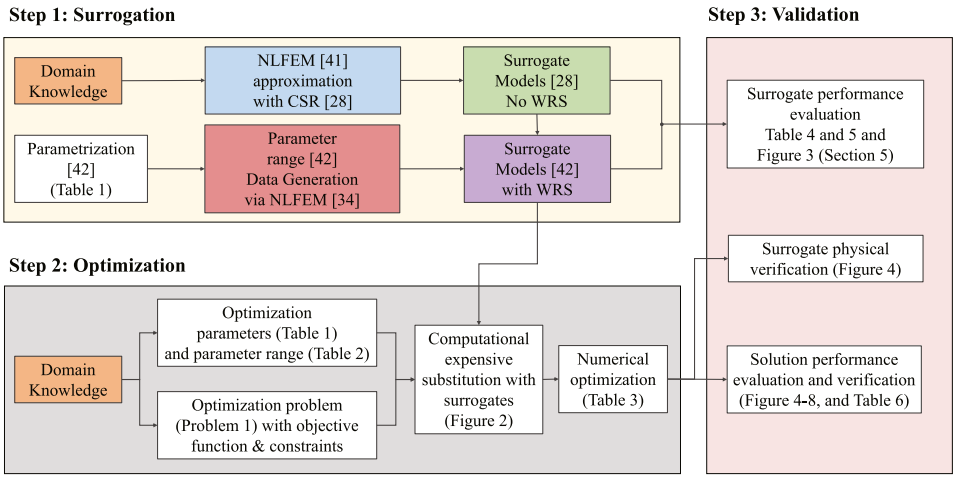

Fig. 1. Graphical representation of the methodology proposed in this work.

welding residual stress is developed. First, authors rely on state-of-the-art analytical approaches coupled with recently data-driven nonlinear finite element methods surrogates characterized by functional which are computationally expensive to build but computationally inexpensive to use. Then, surrogates are used within a design optimization loop to find new optimal designs since nonlinear finite element methods are too computationally demanding for this purpose. Finally, the new designs are reassessed with the original nonlinear finite element methods to verify that substituting them with their surrogates in the optimization loop actually leads to better designs. This methodology is summarized in Fig. 1 and fully described in this section.

3.1. Problem description

Structural optimization of ship structures can be performed on different levels of structural system, namely ship hull girder, cross-stiffened grillage, uni-axially stiffened panel, unstiffened plates, and stiffeners [82]. In this work, authors will focus on structural optimization for uni-axially stiffened panels which are part of a cross-stiffened grillage with uniform longitudinal stiffeners and plating dimension, as depicted in Fig. 2 and adapted from [5,71]. In particular, authors considered a rectangular shaped steel panel reinforced by eight longitudinal stiffeners and surrounded by two main transverse frames and two longitudinal girders (see Dashed red rectangle in Fig. 2). The material yield stress is indicated with σ_Y and Young's modulus with E. In this work, the material is considered fixed, and uniform since a different choice of material grade would significantly influence the overall cost, meaning that this is not the design variable to be considered in the structural optimization of stiffened panels [83]. Considering this geometry, it is possible to define a number of basic geometrical parameters: some of them will be kept fixed while some will be actually optimized. The length between transverse frames a and the distance between longitudinal girders B (i.e., the position of the transverse frames and longitudinal girders) and the distance between the longitudinal stiffeners b (i.e., the number of stiffeners) together with their geometry are considered fixed. In fact, change in the length or the width of stiffened panels may not be driven by the need for minimized weight and maximized strength, but a higher level overarching consideration determined during the early concept design phase (e.g., the general arrangement of ships, subdivision of compartments, productibility, and structural design considerations) other than ULS etc [25]. With respect to the distance between adjacent stiffener (b), there are two main reasons for which it is not considered as a design variable. Firstly, as the overall length of the panel is fixed, there is probably not too much scope to alter the number of stiffeners since the width of local plate should be designed to be compatible with the panel length, i.e., ensuring the aspect ratio of the local plate falls into a reasonable range. Secondly, one of the objectives used in the present optimization is structural weight, as an indicator of the capital expenditure (CAPEX) of engineering design by assuming that cost associated with manufacturing is more or less unchanged among different dimension configurations. However, the change in stiffener number brings an uncertainty as to the manufacturing cost since the required amount of welding is increased/decreased. Thus, the design variables in this paper are confined to plate thickness t_p together with stiffener web height h_w, web thickness t_w, flange width b_f, and flange thickness t_f. Since the present paper is confined to uni-axially stiffened panel optimization, the influence of longitudinal girders and transverse frames (i.e., boundary fixity [84]) will be considered as constant and be approximated as simple support in the FEM verification. On the other hand, the interactive effect with adjacent uni-axially stiffened panels will be considered in the FEM verification by adopting a Two-Span/Two-Bay model in combination with symmetric boundary conditions. This modeling technique is consistent with that recommended in [41] and elaborated in [5,6]. The values of all design variables are reported in Tables 1.

Table 1
Ship-type stiffened panel associated parameters' value.

Parameter	Symbol	Value	Unit	Optimized?
Material yield stress	σ_Y	352.8	[MPa]	
Material Young's modulus	E	205800	[MPa]	
Plate length	a	5120	[mm]	
Panel width	B	8190	[mm]	
Plate width	b	910	[mm]	
Plate thickness	t_p	20	[mm]	✓
Stiffener web height	h_w	598.5	[mm]	✓
Stiffener web thickness	t_w	12	[mm]	✓
Stiffener flange width	b_f	200	[mm]	✓
Stiffener flange thickness	t_f	20	[mm]	✓

In terms of stiffened panel's ULS-based optimization, two indices are relevant: the structural weight W and the ultimate compressive strength σ_{xu} [71,72]. W is simply calculated as the product of the structural volume and the material density. As the material density will be uniform across the entire structure, the structural weight may be represented as the structural volume. σ_{xu} will be evaluated using the CSR approach in [28], however, it should be noted that the CSR method does not account for the detrimental influence of WRS. In order to account also for this phenomenon, the NLFEM needs to be employed [34]. Unfortunately, NLFEM is too computationally expensive and its surrogate need to be employed [42].

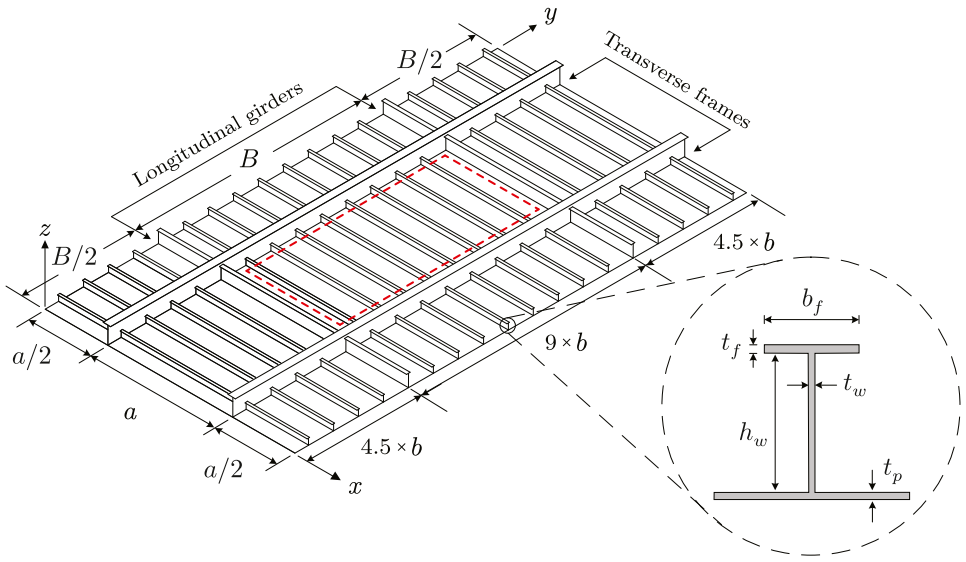

Fig. 2. Ship-type stiffened plated structure representation and associated parameters. Dashed red rectangle indicates the part of the structure that authors will optimize.

Table 2
Design variables and lower/upper bounds.

Parameter	Symbol	Lower bound		Upper bound		Unit
		Symbol	Value	Symbol	Value	
Plate thickness	t_p	t_p^l	8.5	t_p^u	37	[mm]
Stiffener web height	h_w	h_w^l	138	h_w^u	580	[mm]
Stiffener web thickness	t_w	t_w^l	9	t_w^u	15	[mm]
Stiffener flange width	b_f	b_f^l	90	b_f^u	150	[mm]
Stiffener flange thickness	t_f	t_f^l	12	t_f^u	20	[mm]

Obviously, the considered variables can be optimized in a feasible set of values. These constraints, expressed in lower and upper bounds of the design variables [41,50], are summarized in Table 2. In addition to the constraints of Table 2, a manufacture-related constraint is specified, in which the stiffened flange width is constrained to be smaller or equal to the stiffened web height $b_f \leq h_w$. This complies with the conventional practice in the shipbuilding industry [85].

3.2. Problem formalization

According to the problem defined in Section 3.1, authors scope in this paper is to simultaneously optimize the weight W (minimizing it) and the ultimate compressive strength σ_{xu} (maximizing it), considering the WRS, of the structure defined in Fig. 2 optimizing the plate thickness t_p and stiffener web height h_w, web thickness t_w, flange width b_f, and flange thickness t_f with the boundary constraints of Table 2 and the fact that the flange width must be smaller or equal to the stiffened web height $b_f \leq h_w$.

More formally, authors can formulate the following optimization problem

$$\begin{aligned} &\min_{t_p,h_w,t_w,b_f,t_f\in\mathbb{R}} && W(t_p,h_w,t_w,b_f,t_f) \\ &\max_{t_p,h_w,t_w,b_f,t_f\in\mathbb{R}} && \sigma_{xu}(t_p,h_w,t_w,b_f,t_f) \\ &\text{subject to} && \begin{cases} t_p^l \leq t_p \leq t_p^u \\ h_w^l \leq h_w \leq h_w^u \\ t_w^l \leq t_w \leq t_w^u \\ b_f^l \leq b_f \leq b_f^u \\ t_f^l \leq t_f \leq t_f^u \\ b_f \leq h_w. \end{cases} \end{aligned} \tag{1}$$

The expression of $W(t_p,h_w,t_w,b_f,t_f)$ comes out from simple geometrical consideration. In fact the material is homogeneous with constant properties, therefore, the weight is just a function of the volume V and the material's density ρ

$$\begin{aligned} W(t_p,h_w,t_w,b_f,t_f) &= \rho V(t_p,h_w,t_w,b_f,t_f) \\ &= \rho\left[aBt_p + 8a(h_w t_w + b_f t_f)\right]. \end{aligned} \tag{2}$$

The expression of $\sigma_{xu}(t_p,h_w,t_w,b_f,t_f)$ instead is more complex to report and analyze. Without considering the WRS [41]

$$\begin{aligned} &\sigma_{xu}^{\text{NO-WRS-NLFEM}}(t_p,h_w,t_w,b_f,t_f) \\ &= f_{\text{NLFEM}}(\sigma_Y,E,a,B,b,t_p,h_w,t_w,b_f,t_f), \end{aligned} \tag{3}$$

namely, authors can evaluate it using the NLFEM approach proposed in [41]. In order to take into account the WRS authors have to rely on the NLFEM proposed in [34]. Authors will take into account the WRS in the formulation modeling it as a scaling factor of the $f_{\text{NLFEM [41]}}$

$$\begin{aligned} &\sigma_{xu}^{\text{WRS-NLFEM}}(t_p,h_w,t_w,b_f,t_f) \\ &= f_{\text{NLFEM [41]}}(\sigma_Y,E,a,B,b,t_p,h_w,t_w,b_f,t_f) \\ &\quad \cdot f_{\text{NLFEM [34]}}(\sigma_Y,E,a,B,b,t_p,h_w,t_w,b_f,t_f), \end{aligned} \tag{4}$$

namely, the WRS reduces the ultimate compressive strength by a factor of $f_{\text{NLFEM [34]}} \in [0,1]$. $f_{\text{NLFEM [41]}}$ and $f_{\text{NLFEM [34]}}$ computational burden are incompatible with any numerical approach to the solution of the optimization problem of Eq. (1). For this reason authors can approximate first $f_{\text{NLFEM [41]}}$ as follows

$$\begin{aligned} &f_{\text{NLFEM [41]}}(\sigma_Y,E,a,B,b,t_p,h_w,t_w,b_f,t_f) \\ &\approx f_{\text{CSR [28]}}(\sigma_Y,E,a,B,b,t_p,h_w,t_w,b_f,t_f), \end{aligned} \tag{5}$$

namely, using the CSR approach proposed in [28]. As a consequence authors can define

$$\begin{aligned} &\sigma_{xu}^{\text{NO-WRS-CSR}}(t_p,h_w,t_w,b_f,t_f) \\ &= f_{\text{CSR [28]}}(\sigma_Y,E,a,B,b,t_p,h_w,t_w,b_f,t_f), \end{aligned} \tag{6}$$

which is the computationally inexpensive counterpart of $\sigma_{xu}^{\text{NO-WRS-NLFEM}}$. Then, authors can approximate $f_{\text{NLFEM [34]}}$ with the surrogate proposed in [42] obtaining

$$\begin{aligned} &f_{\text{NLFEM [34]}}(\sigma_Y,E,a,B,b,t_p,h_w,t_w,b_f,t_f) \\ &\approx f_{\text{DDM [42]}}(\sigma_Y,E,a,B,b,t_p,h_w,t_w,b_f,t_f). \end{aligned} \tag{7}$$

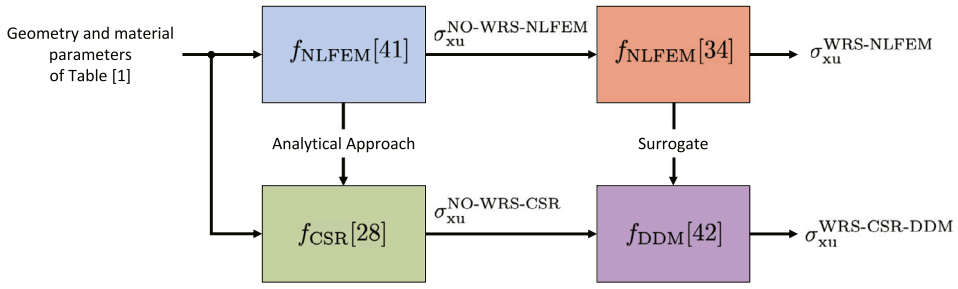

Fig. 3. Authors approach to the accurate yet computational inexpensive estimation of σ_{xu} to employ in the optimization problems of Eq. (1).

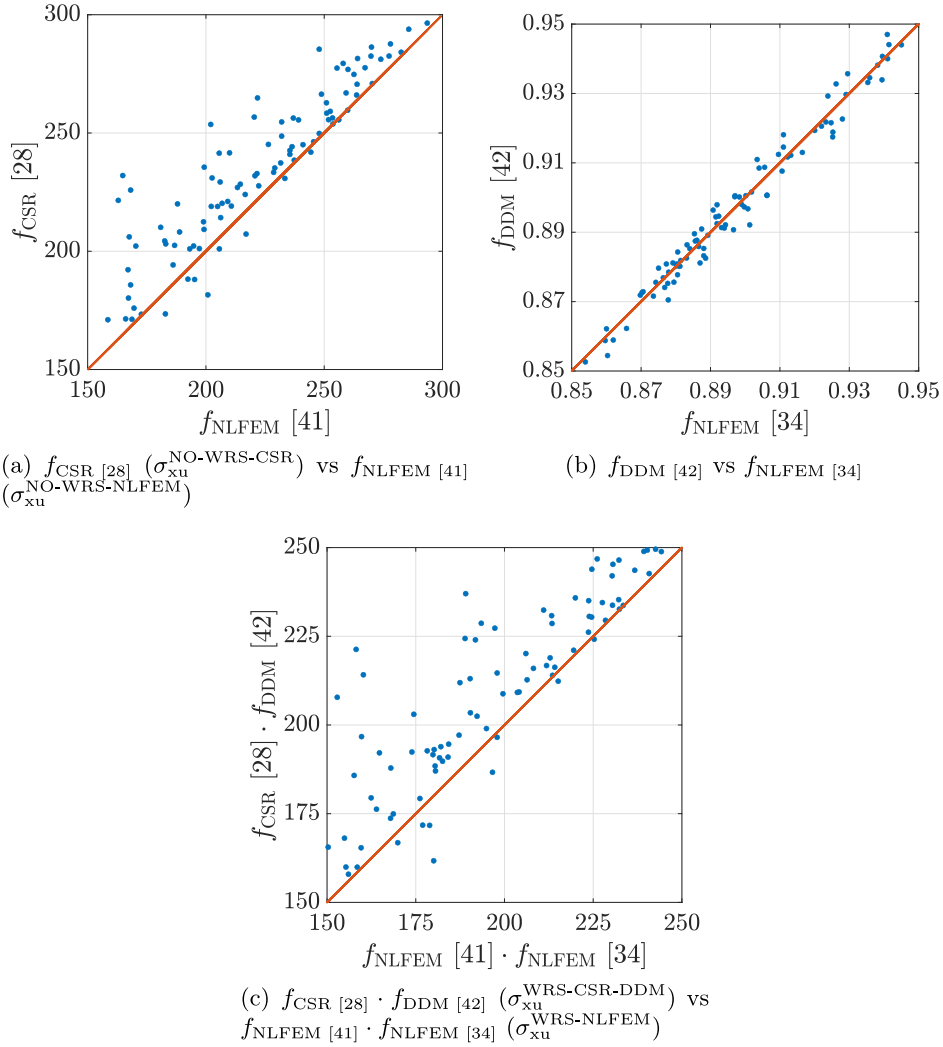

(a) $f_{\text{CSR [28]}}$ $(\sigma_{\text{xu}}^{\text{NO-WRS-CSR}})$ vs $f_{\text{NLFEM [41]}}$ $(\sigma_{\text{xu}}^{\text{NO-WRS-NLFEM}})$

(b) $f_{\text{DDM [42]}}$ vs $f_{\text{NLFEM [34]}}$

(c) $f_{\text{CSR [28]}} \cdot f_{\text{DDM [42]}}$ $(\sigma_{\text{xu}}^{\text{WRS-CSR-DDM}})$ vs $f_{\text{NLFEM [41]}} \cdot f_{\text{NLFEM [34]}}$ $(\sigma_{\text{xu}}^{\text{WRS-NLFEM}})$

Fig. 4. Scatter plots of $f_{\text{CSR [28]}}$ $(\sigma_{\text{xu}}^{\text{NO-WRS-CSR}})$, $f_{\text{DDM [42]}}$, and $f_{\text{CSR [28]}} \cdot f_{\text{DDM [42]}}$ $(\sigma_{\text{xu}}^{\text{WRS-CSR-DDM}})$ against $f_{\text{NLFEM [41]}}$ $(\sigma_{\text{xu}}^{\text{NO-WRS-NLFEM}})$, $f_{\text{NLFEM [34]}}$, and $f_{\text{NLFEM [41]}} \cdot f_{\text{NLFEM [41]}}$ $(\sigma_{\text{xu}}^{\text{WRS-NLFEM}})$ respectively.

As a result, authors proposal is use in the optimization problem of Eq. (1)

$$\begin{aligned}&\sigma_{\text{xu}}^{\text{WRS-CSR-DDM}}(t_p, h_w, t_w, b_f, t_f)\\&= f_{\text{CSR [28]}}(\sigma_Y, E, a, B, b, t_p, h_w, t_w, b_f, t_f)\\&\quad \cdot f_{\text{DDM [42]}}(\sigma_Y, E, a, B, b, t_p, h_w, t_w, b_f, t_f),\end{aligned} \tag{8}$$

which is the computationally inexpensive counterpart of $\sigma_{\text{xu}}^{\text{WRS-NLFEM}}$. To improve the readability of the paper Fig. 3 reports a graphical representation of the approach that authors just described.

Note that this work is the first one proposing to optimize a structure accounting for the WRS. And in this work authors will investigate the changes in the solution of the optimization problems of Eq. (1) replacing σ_{xu} with $\sigma_{\text{xu}}^{\text{NO-WRS-CSR}}$, $\sigma_{\text{xu}}^{\text{WRS-NLFEM}}$, and finally $\sigma_{\text{xu}}^{\text{WRS-DDM}}$.

3.3. Problem resolution

The first step toward the solution of Eq. (1) is to reformulate the problem as a single objective one. For this purpose authors will rely on a classical approach: replace the multiple objectives with a weighted sum of the different objectives (changing the sign in front to the objective so as to have all minimization or maximization) [86]

$$\min_{t_p, h_w, t_w, b_f, t_f \in \mathbb{R}} \quad \lambda V(t_p, h_w, t_w, b_f, t_f) - (1-\lambda)\sigma_{\text{xu}}(t_p, h_w, t_w, b_f, t_f) \tag{9}$$

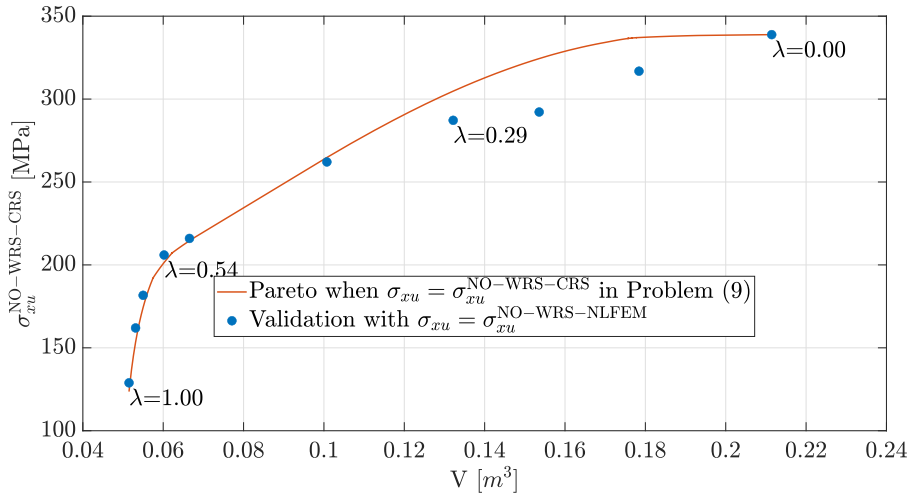

(a) $\sigma_{\text{xu}} = \sigma_{\text{xu}}^{\text{NO-WRS-CSR}}$ in Eq. (9).

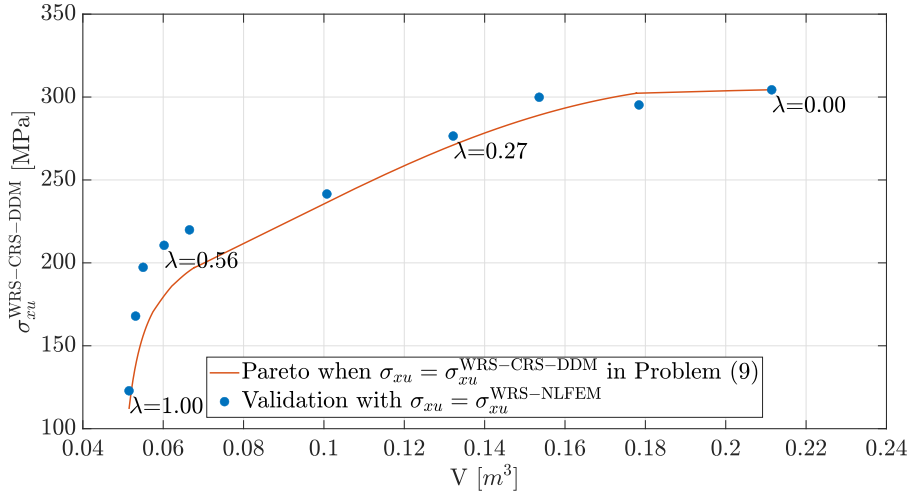

(b) $\sigma_{\text{xu}} = \sigma_{\text{xu}}^{\text{WRS-CSR-DDM}}$ in Eq. (9).

Fig. 5. Optimal V and the optimal σ_{xu} varying λ in Eq. (9) creating the Pareto fronts when replacing replace σ_{xu} with $\sigma_{\text{xu}}^{\text{NO-WRS-CSR}}$ or $\sigma_{\text{xu}}^{\text{WRS-CSR-DDM}}$. For some λs (i.e., the ones that brings a particular optimal volume $V \in [0.2114, 0.1322, 0.0602, 0.0515]$) authors reported for verification purposes at the optimal point the $\sigma_{\text{xu}}^{\text{NO-WRS-NLFEM}}$ when $\sigma_{\text{xu}} = \sigma_{\text{xu}}^{\text{NO-WRS-CSR}}$ is exploited in Eq. (9) and $\sigma_{\text{xu}}^{\text{WRS-NLFEM}}$ when $\sigma_{\text{xu}} = \sigma_{\text{xu}}^{\text{WRS-CSR-DDM}}$ is exploited in Eq. (9).

$$\text{subject to} \quad \begin{cases} t_p^l \le t_p \le t_p^u \\ h_w^l \le h_w \le h_w^u \\ t_w^l \le t_w \le t_w^u \\ b_f^l \le b_f \le b_f^u \\ t_f^l \le t_f \le t_f^u \\ b_f \le h_w, \end{cases}$$

where authors replaced W with V since there are proportional and where $\lambda \in [0, 1]$ defines the importance of the different objectives, i.e., for $\lambda \to 1$ authors care more about the weight than the ultimate compressive strength and vice-versa for $\lambda \to 0$. Solving Eq. (9) for different values of λ allows for the creation of the so-called Pareto frontier in a computationally efficient way [86].

The optimization problem of Eq. (9) has a non-linear and non-convex objective (no matter if authors replace σ_{xu} with $\sigma_{\text{xu}}^{\text{NO-WRS-CSR}}$ or $\sigma_{\text{xu}}^{\text{WRS-CSR-DDM}}$) and a series of linear constraints (namely the domain is linear and convex). In order to solve this problem different approaches can be exploited [87]. In this paper, authors will rely on a series of state-of-the-art optimization algorithms to search for the best one for authors specific problem. In fact, a series of no-free-lunch theorems [88] ensure that there is no way to choose a-priori the best optimization algorithms for a particular problem and the only options is to empirically test multiple approaches verifying which is actually the best one. In this case, authors decided to test the following algorithms: the Interior-Point (IP) [45], the Active-Set (AS) [46], the Genetic Algorithm (GA) [47], and the Particle Swarm Optimization (PSO) [48]. The different algorithms are characterized by a different search strategy, a different way of handling constraints or are inspired by a different philosophy. To the best knowledge of the authors, and based on the recent literature [87], these optimization algorithms reasonably cover the most important approaches to the solution of the optimization problem of Eq. (9). Since the convergence of all these algorithms is influenced by the starting point, a multi-start strategy [89] for all methods has been employed. In particular, as starting point, authors used: (i) the initial geometry described in Table 1 and (ii) 100 random points uniformly distributed in the domain induced by the linear constraints of the optimization problem of Eq. (9). The optimization methods have been implemented using the Matlab 2022a[1] environment. Table 3 summarizes the parameter setting of the different algorithms.

[1] https://www.mathworks.com/

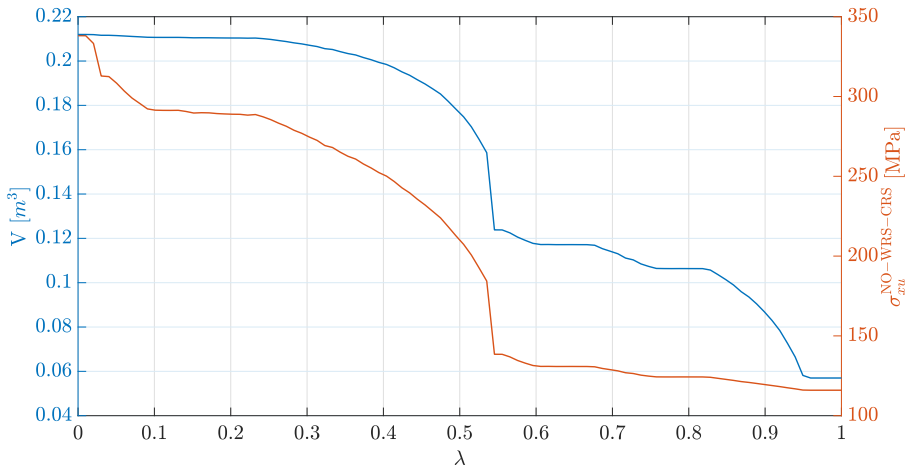

(a) $\sigma_{xu} = \sigma_{xu}^{\text{NO-WRS-CSR}}$ in Eq. (9).

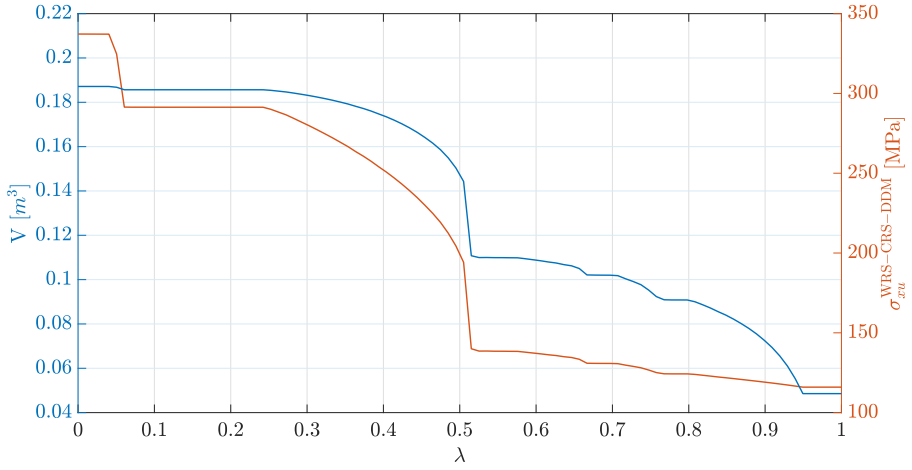

(b) $\sigma_{xu} = \sigma_{xu}^{\text{WRS-CSR-DDM}}$ in Eq. (9).

Fig. 6. Optimal V and the optimal σ_{xu} varying λ in Eq. (9) when authors replace σ_{xu} with $\sigma_{xu}^{\text{NO-WRS-CSR}}$ or $\sigma_{xu}^{\text{WRS-CSR-DDM}}$ in a different manner with respect to Fig. 5 so to better understand how V and σ_{xu} varies with λ.

Table 3
Parameters setting for the different optimization algorithms.

Algorithm	Matlab function	Parameter	Value(s)
IP	fmincon	Algorithm	interior-point
		Maximum number of function evaluations allowed	10^6
		Maximum number of iterations allowed	10^5
AS	fmincon	Algorithm	active-set
		Maximum number of function evaluations allowed	10^6
		Maximum number of iterations allowed	10^5
		Maximum number of SQP iterations allowed	600
GA	ga	Population size	5000
		Elite count	250
PSO	particleswarm	Swarm size	5000
		Maximum number of iterations	1000

Finally, authors would like to discuss how to handle the optimization problem of Eq. (9) when authors replace σ_{xu} with $\sigma_{xu}^{\text{NO-WRS-CSR}}$ or $\sigma_{xu}^{\text{WRS-CSR-DDM}}$. When authors want to optimize the weight and the ultimate compressive strength not taking into account the WRS authors have to replace σ_{xu} with $\sigma_{xu}^{\text{NO-WRS-CSR}}$ in Eq. (9) and the resulting optimization problem can be directly handled with the optimizers described in the previous paragraph since estimating $\sigma_{xu}^{\text{NO-WRS-CSR}}$ is computationally inexpensive. Then, once the optimization problem of Eq. (9) with $\sigma_{xu} = \sigma_{xu}^{\text{NO-WRS-CSR}}$ is solved authors need to estimate, in the optimal point, the actual value of $\sigma_{xu}^{\text{NO-WRS-NLFEM}}$ (i.e., just one estimation) to verify that the surrogate is actually a good hint for the optimizer and bring the solution to point when the original function is actually optimized and does not introduces artifacts or false minima.

Instead, in the case, authors want to optimize the weight and the ultimate compressive strength taking into account the WRS authors have to replace σ_{xu} with $\sigma_{xu}^{\text{WRS-CSR-DDM}}$ in Eq. (9). Then, once the optimization problem of Eq. (9) with $\sigma_{xu} = \sigma_{xu}^{\text{WRS-CSR-DDM}}$ is solved it is necessary to estimate, in the optimal point, the actual value of $\sigma_{xu}^{\text{WRS-NLFEM}}$ (i.e., just one estimation) to verify that the surrogate is actually a good hint for

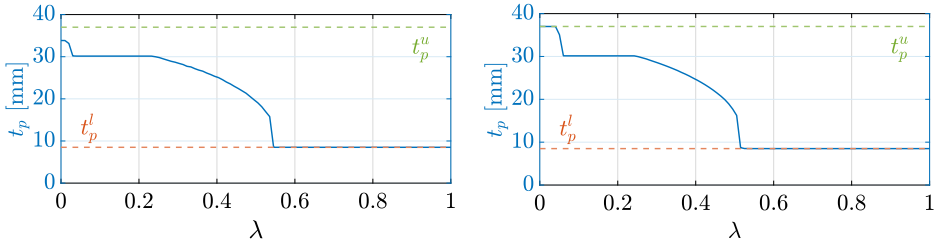

(a) t_p when σ_{xu}=$\sigma_{\text{xu}}^{\text{NO-WRS-CSR}}$ in Eq. (9). (b) t_p when σ_{xu}=$\sigma_{\text{xu}}^{\text{WRS-CSR-DDM}}$ in Eq. (9).

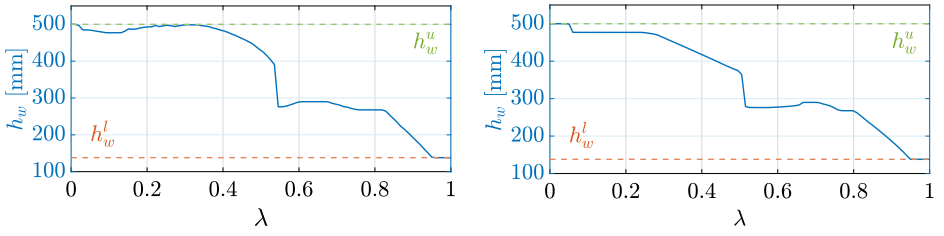

(c) h_w when σ_{xu}=$\sigma_{\text{xu}}^{\text{NO-WRS-CSR}}$ in Eq. (9). (d) h_w when σ_{xu}=$\sigma_{\text{xu}}^{\text{WRS-CSR-DDM}}$ in Eq. (9).

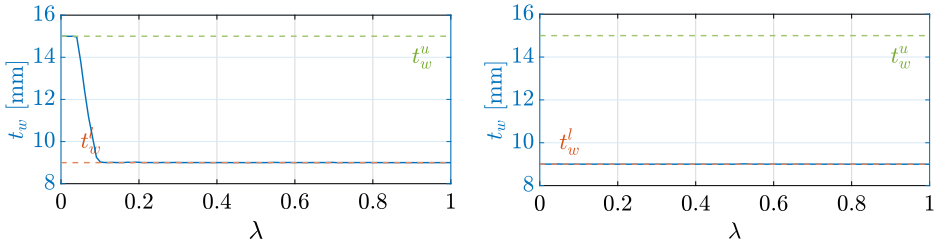

(e) t_w when σ_{xu}=$\sigma_{\text{xu}}^{\text{NO-WRS-CSR}}$ in Eq. (9). (f) t_w when σ_{xu}=$\sigma_{\text{xu}}^{\text{WRS-CSR-DDM}}$ in Eq. (9).

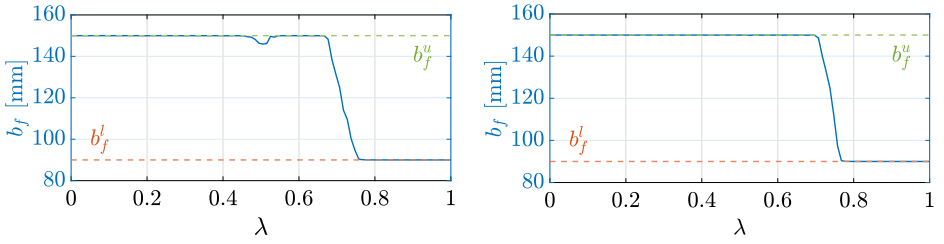

(g) b_f when σ_{xu}=$\sigma_{\text{xu}}^{\text{NO-WRS-CSR}}$ in Eq. (9). (h) b_f when σ_{xu}=$\sigma_{\text{xu}}^{\text{WRS-CSR-DDM}}$ in Eq. (9).

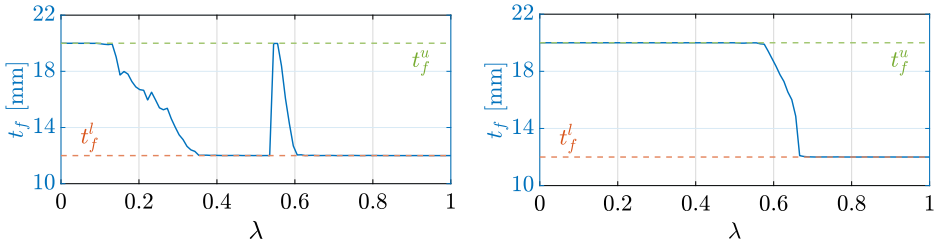

(i) t_f when σ_{xu}=$\sigma_{\text{xu}}^{\text{NO-WRS-CSR}}$ in Eq. (9). (j) t_f when σ_{xu}=$\sigma_{\text{xu}}^{\text{WRS-CSR-DDM}}$ in Eq. (9).

Fig. 7. Optimized variables (t_p, h_w, t_w, b_f, and t_f) behavior when varying λ in Eq. (9) replacing σ_{xu} with $\sigma_{\text{xu}}^{\text{NO-WRS-CSR}}$ or $\sigma_{\text{xu}}^{\text{WRS-CSR-DDM}}$.

the optimizer and bring the solution to point when the original function is actually optimized and does not introduces artifacts or false minima.

The verification are, in fact, fundamental. Firstly, this approach enables an indirect examination of the efficacy of the surrogate models $\sigma^{\text{NO-WRS-CSR}}$xu and $\sigma^{\text{WRS-CSR-DDM}}$xu in approximating the actual $\sigma^{\text{NO-WRS-NLFEM}}$xu and $\sigma^{\text{WRS-NLFEM}}$xu, respectively. The strength of surrogate models lies in their potential to be employed in contexts that extend beyond the design conditions initially set for the surrogate itself. This ability to effectively extrapolate is an important characteristic of a robust surrogate model. Consequently, assessing this extrapolation power provides insight into the surrogate's adaptability and reliability in diverse scenarios, thereby providing a measure of its overall extrapolating power [42]. Second, it allows us to directly verify that authors proposal is actually grounded and effective.

4. Experimental results

In this section, authors will show the results of applying the solution in Section 3.2 to the problem described in Section 3.1.

Table 4
Errors, measured with the MAE, MAPE, and PMCC, of $f_{\text{CSR [28]}}$ ($\sigma_{xu}^{\text{NO-WRS-CSR}}$), $f_{\text{DDM [42]}}$, and $f_{\text{CSR [28]}} \cdot f_{\text{DDM [42]}}$ ($\sigma_{xu}^{\text{WRS-CSR-DDM}}$) in estimating $f_{\text{NLFEM [41]}}$ ($\sigma_{xu}^{\text{NO-WRS-NLFEM}}$), $f_{\text{NLFEM [34]}}$, and $f_{\text{NLFEM [41]}} \cdot f_{\text{NLFEM [34]}}$ ($\sigma_{xu}^{\text{WRS-NLFEM}}$) respectively.

Original Model	Surrogate	MAE	MAPE	PPMCC
$f_{\text{NLFEM [41]}}$	$f_{\text{CSR [28]}}$	15.71	8.25	0.91
$f_{\text{NLFEM [34]}}$	$f_{\text{DDM [42]}}$	0.003	0.34	0.99
$f_{\text{NLFEM [41]}} \cdot f_{\text{NLFEM [34]}}$	$f_{\text{CSR [28]}} \cdot f_{\text{DDM [42]}}$	14.40	8.24	0.88

Table 5
Average time necessary to make a prediction for the different models: $\sigma_{xu}^{\text{NO-WRS-NLFEM}}$, $\sigma_{xu}^{\text{WRS-NLFEM}}$, $\sigma_{xu}^{\text{NO-WRS-CSR}}$, and $\sigma_{xu}^{\text{WRS-CSR-DDM}}$.

Model	Average time [s]
$\sigma_{xu}^{\text{NO-WRS-NLFEM}}$	$1.8 \cdot 10^3$
$\sigma_{xu}^{\text{WRS-NLFEM}}$	$3.6 \cdot 10^3$
$\sigma_{xu}^{\text{NO-WRS-CSR}}$	9
$\sigma_{xu}^{\text{WRS-CSR-DDM}}$	9

Table 6
Average number of calls and the average time that each optimization algorithm (IP, AS, GA, or PSO) take in finding the solution when replacing σ_{xu} with $\sigma_{xu}^{\text{NO-WRS-CSR}}$ or $\sigma_{xu}^{\text{WRS-CSR-DDM}}$ in the optimization problem of Eq. (9).

	Algorithm	Average calls [n^o]	Average time [s]
$\sigma_{xu}^{\text{NO-WRS-CSR}}$	AS	197	0.035
	IP	571	0.152
	PSO	1305	0.98
	GA	8600	89.5
$\sigma_{xu}^{\text{WRS-CSR-DDM}}$	AS	187	0.067
	IP	559	0.267
	PSO	1194	0.93
	GA	7239	96.5

As a first step, Table 4 reports the accuracy of the Analytical Approach and the Data Driven based surrogate models (see Fig. 3). In particular, authors report the errors of $f_{\text{CSR [28]}}$ ($\sigma_{xu}^{\text{NO-WRS-CSR}}$) in estimating $f_{\text{NLFEM [41]}}$ ($\sigma_{xu}^{\text{NO-WRS-NLFEM}}$), then the one of $f_{\text{DDM [42]}}$ in estimating $f_{\text{NLFEM [34]}}$, and finally the one of $f_{\text{CSR [28]}} \cdot f_{\text{DDM [42]}}$ ($\sigma_{xu}^{\text{WRS-CSR-DDM}}$) in estimating $f_{\text{NLFEM [41]}} \cdot f_{\text{NLFEM [34]}}$ ($\sigma_{xu}^{\text{WRS-NLFEM}}$). In order to give a quantitative idea of the quality of the results, authors used three metrics [90]: the Mean Average Error (MAE), the Mean Average Percentage Error (MAPE), and the Pearson Product Moment Correlation Coefficient (PPMCC). Note that authors measure these errors as the one described in [42]. For completeness, authors also report the scatter plots (Analytical Approaches and the Data Driven based surrogate models) in Fig. 4 to provide a visual and qualitative idea [91] of the effectiveness of the different estimations. Finally, Table 5 reports the average time necessary to make a prediction for the different considered models ($\sigma_{xu}^{\text{NO-WRS-NLFEM}}$, $\sigma_{xu}^{\text{WRS-NLFEM}}$, $\sigma_{xu}^{\text{NO-WRS-CSR}}$, and $\sigma_{xu}^{\text{WRS-CSR-DDM}}$).

From Table 4 and Fig. 4 it is possible to observe a good agreement between the Analytical Approach and the Data Driven based surrogate models and the original models. In particular, the Data Driven based surrogate models are very effective with MAPE error below 1% as expected from [42], while the Analytical Approach (i.e., CSR) shows a MAPE error below 10% most of the time with an overestimation as expected from [41,92]. The overestimation should be attributed to the use of the Frankland formula [93] in CSR as performance measure to evaluate the effectiveness of a buckled plate based on an effective width concept. However, the Frankland formula was developed based on collapse test data of fully restrained plates and hence tends to overestimate the capacity due to the consideration of pull-in effect in comparison, e.g., with Faulkner formula [82]. In actual stiffened panel structures, the boundary conditions (i.e., edge fixity) are neither fully restrained nor free from constraint, but in between zero and infinite edge fixity, and are the complex resultant of the interaction with adjacent structures. The present NLFEM is able to accommodate this interacting phenomenon since a Two-Span/Two-Bay model is adopted [42]. Nevertheless, the restrained edge assumption and, thus, the overestimation is built into the CSR [28]. From Table 5, instead, it is possible to observe how the CSR and the Data Driven based surrogate models are orders of magnitude faster than the NLFEM models. In this case, the CSR brings the computational effort from minutes to seconds while the DDM adds to the CSR a negligible contribution (milliseconds). This is an encouraging feature since it demonstrates that the computational efficiency of CSR is retained, which is one of the core benefits of Analytical Approach. Thus, this approach remains suitable for the ordinary structural design of stiffened plated structures.

As a second step, authors consider the optimization problem of Eq. (9) when authors replace σ_{xu} with $\sigma_{xu}^{\text{NO-WRS-CSR}}$ or $\sigma_{xu}^{\text{WRS-CSR-DDM}}$. In particular, in Fig. 5 authors report the optimal V and the optimal σ_{xu} varying λ in Eq. (9) creating the Pareto fronts when replacing replace σ_{xu} with $\sigma_{xu}^{\text{NO-WRS-CSR}}$ or $\sigma_{xu}^{\text{WRS-CSR-DDM}}$. Moreover, for some λs (i.e., the ones that brings a particular optimal volume $V \in [0.2114, 0.1322, 0.0602, 0.0515]$) authors reported for verification purposes at the optimal point, also the $\sigma_{xu}^{\text{NO-WRS-NLFEM}}$ when $\sigma_{xu} = \sigma_{xu}^{\text{NO-WRS-CSR}}$ is exploited in Eq. (9) and $\sigma_{xu}^{\text{WRS-NLFEM}}$ when $\sigma_{xu} = \sigma_{xu}^{\text{WRS-CSR-DDM}}$ is exploited in Eq. (9). Fig. 5 clearly shows that the Pareto front reasonably correlates with the NLFEM predictions. Additionally, it is possible to observe that the structural strength of the stiffened panel considered in this paper is insensitive to the change in structural geometry/weight when it is already designed to be stocky. This is probably due to the structural behavior in these cases are dominated by material plasticity rather than structural instability (i.e., buckling). In contrast, the structural strength of the stiffened panel considered is highly sensitive to the change in structural geometry/weight when it is designed to be slender. This can be attributed to the fact that the dominating buckling mode in these cases is changed from elastoplastic local plate buckling to elastic stiffener tripping and/or overall single-frame buckling. The above observations suggest that it is important for structural designers to identify the turning points in a Pareto front since changing the geometry of a stocky stiffened panel can be a benefit (decreasing structural weight without a significant sacrifice of structural performance), whereas the structural performance can be considerably degraded even with a change in geometry for slender panels. Fig. 6 reports the optimal V and the optimal σ_{xu} varying λ in Eq. (9) when authors replace σ_{xu} with $\sigma_{xu}^{\text{NO-WRS-CSR}}$ or $\sigma_{xu}^{\text{WRS-CSR-DDM}}$ differently with respect to Fig. 5 so to better understand how V and σ_{xu} varies with λ. Fig. 7, instead, reports how the optimized variables (t_p, h_w, t_w, b_f, and t_f) behavior when varying λ in Eq. (9) replacing σ_{xu} with $\sigma_{xu}^{\text{NO-WRS-CSR}}$ or $\sigma_{xu}^{\text{WRS-CSR-DDM}}$. Figs. 8 and 9 reports, for some λs (the same of Fig. 5, namely the ones that brings a particular optimal volume $V \in [0.2114, 0.1322, 0.0602, 0.0515]$) a visualization of the geometry found with the optimization problem of Eq. (9) when authors replace σ_{xu} with $\sigma_{xu}^{\text{NO-WRS-CSR}}$ or $\sigma_{xu}^{\text{WRS-CSR-DDM}}$ respectively against the original geometry of Table 1. It is noted from Fig. 6 that when $\lambda > 0.5$, structural strength and structural weight substantially reduce. This is primarily driven by the greater importance of structural weight minimization which outweighs the structural strength maximization. Furthermore, with reference to Fig. 7, the plate thickness (t_p) and the stiffener height (h_w) appears to be the two most influencing parameters as shown by their variation relations against λ which show a close match with the change of structural weight and strength against varying λ. This aligns with many parametric analyses of the strength of stiffened plated structures [40,41]. The change in the plate thickness causes the largest difference in the structural performance since the local plate is the major part (in terms of material volume) of a stiffened plated structure and thereby plays a prime role in providing the load-carrying capacity. On the other hand, the role of the stiffener is to provide boundary support to the local plating to prevent the stiffened panel from overall buckling failure. In particular, the stiffener height would dictate the fixity of the boundary constraint and whether any stiffener tripping would occur, in which case a significant loss in boundary constraint would result.

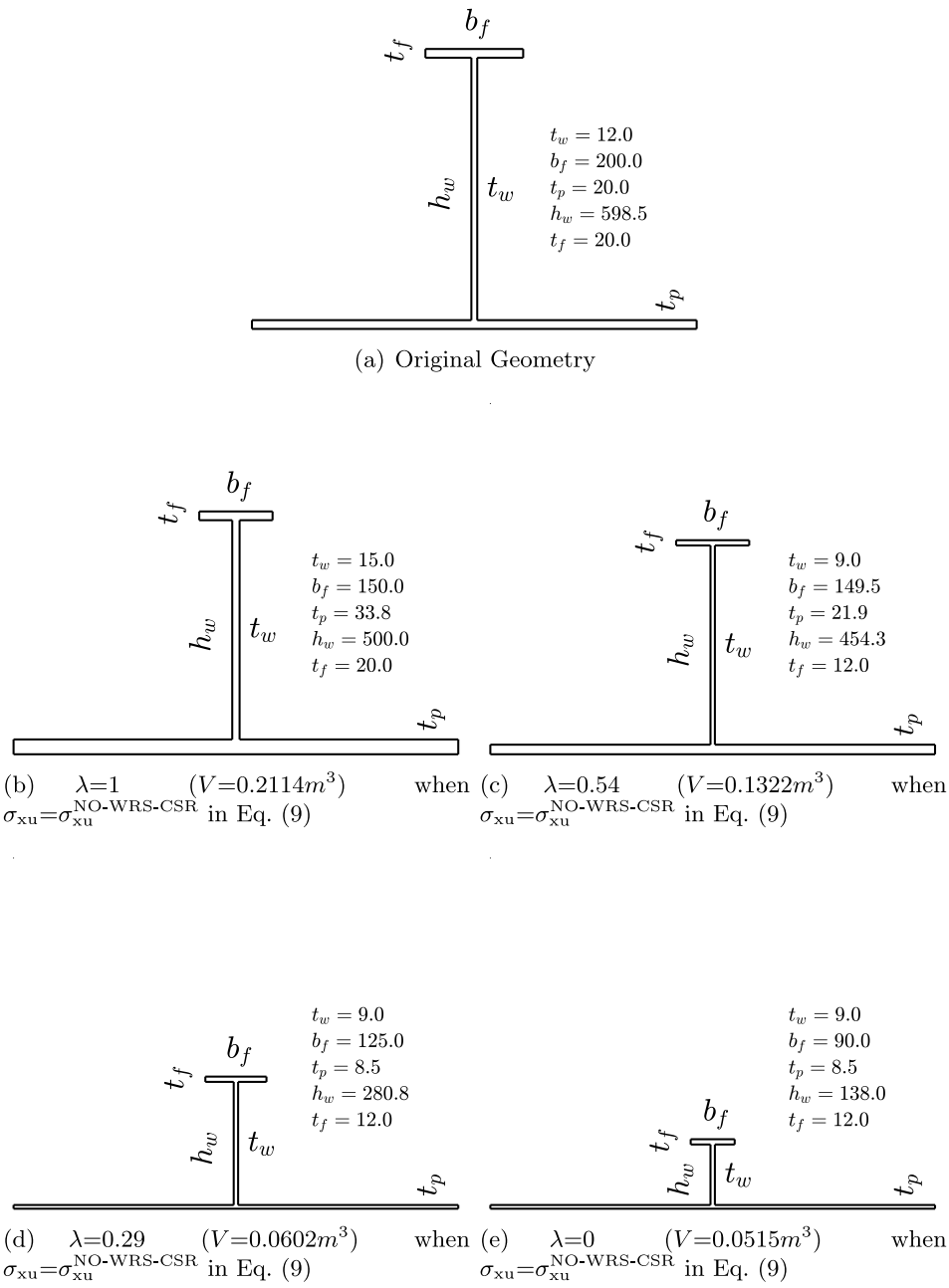

(a) Original Geometry

(b) λ=1 (V=0.2114m^3) when σ_{xu}=$\sigma_{xu}^{\text{NO-WRS-CSR}}$ in Eq. (9)

(c) λ=0.54 (V=0.1322m^3) when σ_{xu}=$\sigma_{xu}^{\text{NO-WRS-CSR}}$ in Eq. (9)

(d) λ=0.29 (V=0.0602m^3) when σ_{xu}=$\sigma_{xu}^{\text{NO-WRS-CSR}}$ in Eq. (9)

(e) λ=0 (V=0.0515m^3) when σ_{xu}=$\sigma_{xu}^{\text{NO-WRS-CSR}}$ in Eq. (9)

Fig. 8. For some λs (the same of Fig. 5, namely the ones that brings a particular optimal volume $V \in [0.2114, 0.1322, 0.0602, 0.0515]$) authors report a visualization of the geometry found with the optimization problem of Eq. (9) when authors replace σ_{xu} with $\sigma_{xu}^{\text{NO-WRS-CSR}}$ against the original geometry of Table 1.

Note that in all the results presented before, authors did not specify the optimization algorithm exploited (IP, AS, GA, or PSO) since they all find the same optimal solution. Since the solution's optimality cannot be a criterion for selecting the best optimization algorithm, authors will use their computational requirements as a metric to compare them. For this reason, Table 6 reports the average number of calls and the average time that each optimization algorithm takes to find the solution when replacing σ_{xu} with $\sigma_{xu}^{\text{NO-WRS-CSR}}$ or $\sigma_{xu}^{\text{WRS-CSR-DDM}}$ in the optimization problem of Eq. (9).

From Table 6, it is clear that AS is the best suited candidate for the problem at hand since IP, PSO, and GA are an order of magnitude slower than AS.

5. Conclusions

Modern structures are usually designed as a network of plates and stiffeners joined by welding, which induces a residual stress field, and their design is a long process of adaptation of existing structures not optimized for the specific requirements, resulting in being overly conservative. A design able to simultaneously minimize the weight and maximize the strength of the panels would result in technical, economic, and environmental benefits. Given the geometry, computing the weight of the panel is trivial, while estimating its strength is not trivial at all, both from methodological and technical sides. In fact, ultimate limit state assessment examines the maximum load-carrying capacity of

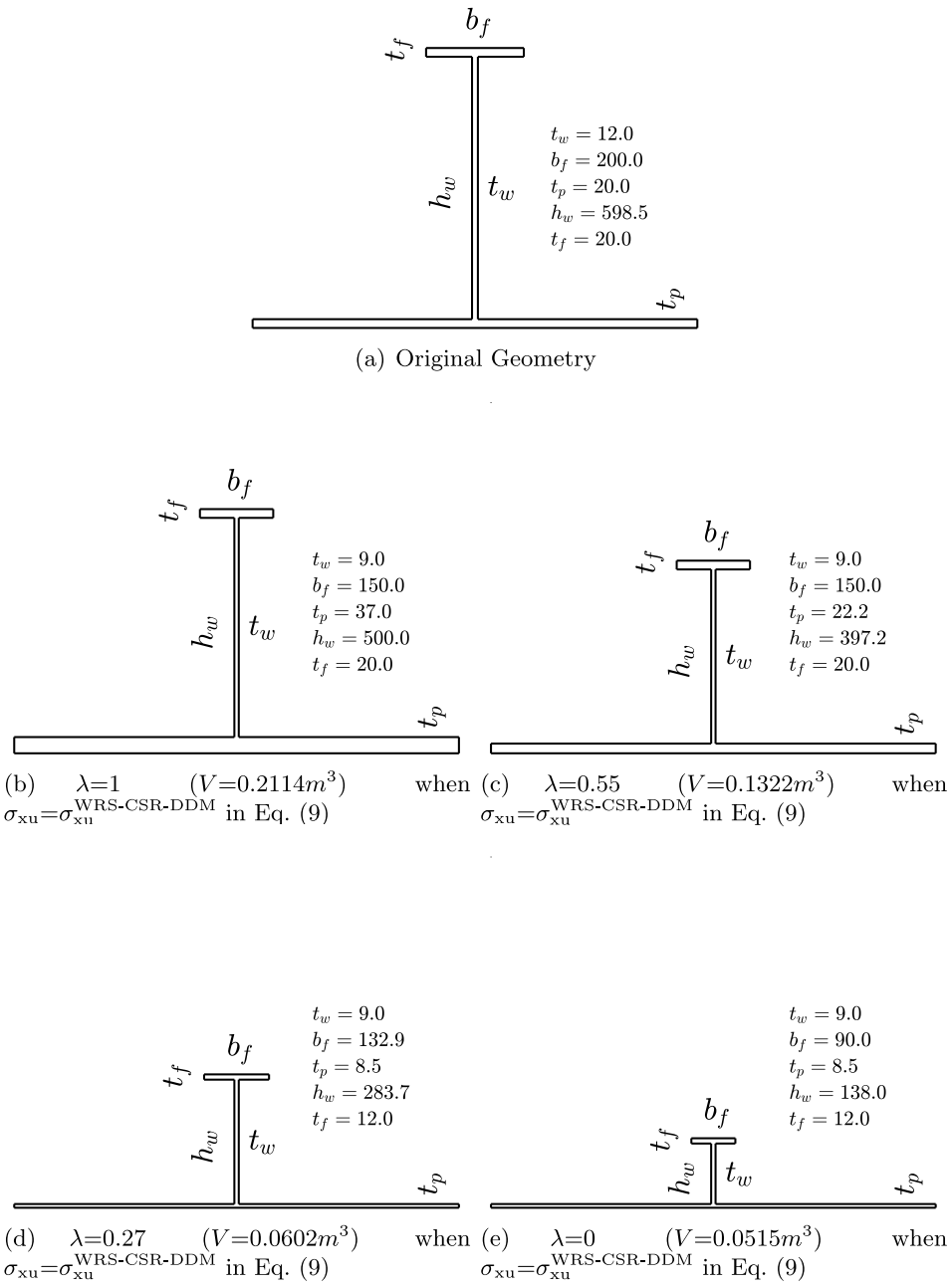

(a) Original Geometry

(b) λ=1 (V=0.2114m^3) when σ_{xu}=$\sigma_{xu}^{\text{WRS-CSR-DDM}}$ in Eq. (9)

(c) λ=0.55 (V=0.1322m^3) when σ_{xu}=$\sigma_{xu}^{\text{WRS-CSR-DDM}}$ in Eq. (9)

(d) λ=0.27 (V=0.0602m^3) when σ_{xu}=$\sigma_{xu}^{\text{WRS-CSR-DDM}}$ in Eq. (9)

(e) λ=0 (V=0.0515m^3) when σ_{xu}=$\sigma_{xu}^{\text{WRS-CSR-DDM}}$ in Eq. (9)

Fig. 9. For some λs (the same of Fig. 5, namely the ones that brings a particular optimal volume $V \in [0.2114, 0.1322, 0.0602, 0.0515]$) authors report a visualization of the geometry found with the optimization problem of Eq. (9) when authors replace σ_{xu} with $\sigma_{xu}^{\text{WRS-CSR-DDM}}$ against the original geometry of Table 1.

structures considering inelastic buckling failure and, to provide reliable assessments, needs to take into account also the stress induced by the welding, namely the welding residual stress. Effectively predicting the ultimate limit state reduction of stiffened panels accounting also for the welding residual stress requires the use of nonlinear finite element methods, which are too computationally demanding to be used in a design optimization loop. For this reason, in this paper, a three-step approach for the optimal design of stiffened panels accounting for ultimate limit state due to welding residual stress is developed. First, authors rely on state-of-the-art Analytical Approaches coupled with recently data-driven nonlinear finite element methods surrogates characterized by functional, which are computationally expensive to build but computationally inexpensive to use. Then, the surrogates are used within a design optimization loop to find new optimal designs. Finally, the new designs are reassessed with the original nonlinear finite element methods to verify that substituting the nonlinear finite element methods with their surrogates in the optimization loop leads to better designs. Results obtained optimizing a series of parameters of a commonly used stiffened panel geometry under different scenarios supported authors proposal. A number of research areas may be open for future study. To ensure a more reliable design optimization, continuing efforts on the improvement of prediction methods for ultimate strength of stiffened plated structures including analytical and surrogate models are required. Additionally, probabilistic analysis can be performed to deal with the uncertainty related to strength prediction. Combining the probabilistic analysis with the proposed optimization framework, a reliability-based structural optimization may be investigated. Further, additional design variables may be introduced and the objective functional can be modified to consider a techno-economic optimization.

CRediT authorship contribution statement

Andrea Coraddu: Conceptualization, Methodology, Software, Validation, Data curation, Supervision, Writing – original draft, Writing – reviewing & editing. **Luca Oneto:** Conceptualization, Methodology, Software, Validation, Data curation, Supervision, Writing – original draft, Writing – reviewing & editing. **Shen Li:** Conceptualization, Methodology, Software, Validation, Data curation, Supervision, Writing – original draft, Writing – reviewing & editing. **Miltiadis Kalikatzarakis:** Methodology, Software, Writing – original draft. **Olena Karpenko:** Conceptualization, Methodology, Writing – original draft, Writing – reviewing & editing.

Declaration of competing interest

The authors declare that they have no known competing financial interests or personal relationships that could have appeared to influence the work reported in this paper.

Data availability

Data will be made available on request.

References

[1] Paik JK. Ultimate limit state analysis and design of plated structures. Wiley Online Library; 2018, http://dx.doi.org/10.1002/9781119367758.

[2] Sechler EE, G. DL. Airplane structural analysis and design. John Wiley & Sons; 1944, https://archive.org/details/in.ernet.dli.2015.205355/page/n87/mode/2up.

[3] Paik JK. Advanced structural safety studies: with extreme conditions and accidents. Springer; 2020, http://dx.doi.org/10.1007/978-981-13-8245-1.

[4] Kim TS, Kuwamura H, Kim SH, Lee YT, Cho TJ. Investigation on ultimate strength of thin-walled steel single shear bolted connections with two bolts using finite element analysis. Thin-Walled Struct 2009;47:1191–202. http://dx.doi.org/10.1016/j.tws.2009.04.009.

[5] Kim DK, Lim HL, Kim MS, Hwang OJ, Park KS. An empirical formulation for predicting the ultimate strength of stiffened panels subjected to longitudinal compression. Ocean Eng 2017;140:270–80. http://dx.doi.org/10.1016/j.oceaneng.2017.05.031.

[6] Kim DK, Lim HL, Yu SY. Ultimate strength prediction of T-bar stiffened panel under longitudinal compression by data processing: A refined empirical formulation. Ocean Eng 2019;192:106522. http://dx.doi.org/10.1016/j.oceaneng.2019.106522.

[7] Kim DK, Yu SY, Lim HL, Cho NK. Ultimate compressive strength of stiffened panel: An empirical formulation for flat-bar type. J Mar Sci Eng 2020;8:605. http://dx.doi.org/10.3390/jmse8080605.

[8] Jia JB, Paik JK. Engineering dynamics and vibrations. CRC Press; 2018, http://dx.doi.org/10.1201/9781315119908.

[9] Kim DK, Incecik A, Choi HS, Wong EWC, Yu SY, Park KS. A simplified method to predict fatigue damage of offshore riser subjected to vortex-induced vibration by adopting current index concept. Ocean Eng 2018;157:401–11. http://dx.doi.org/10.1016/j.oceaneng.2018.03.042.

[10] Yu ZL, Amdahl J, Sha YY. Large inelastic deformation resistance of stiffened panels subjected to lateral loading. Mar Struct 2018;59:342–67. http://dx.doi.org/10.1016/j.marstruc.2018.01.005.

[11] Li S, Hu ZQ, Benson S. An analytical method to predict the buckling and collapse behaviour of plates and stiffened panels under cyclic loading. Eng Struct 2019;109627. http://dx.doi.org/10.1016/j.engstruct.2019.109627.

[12] Li S, Kim DK, Benson S. A probabilistic approach to assess the computational uncertainty of ultimate strength of hull girders. Reliab Eng Syst Saf 2021;107688. http://dx.doi.org/10.1016/j.ress.2021.107688.

[13] Li S, Hu ZQ, Benson S. Progressive collapse analysis of ship hull girders subjected to extreme cyclic bending. Mar Struct 2020;102803. http://dx.doi.org/10.1016/j.marstruc.2020.102803.

[14] Li S, Kim DK. Ultimate strength characteristics of unstiffened cylindrical shell in axial compression. Ocean Eng 2022;243:110253. http://dx.doi.org/10.1016/j.oceaneng.2021.110253.

[15] Yao T, Fujikubo M. Buckling and ultimate strength of ship and ship-like floating structures. Butterworth-Heinemann; 2016, http://dx.doi.org/10.1016/C2015-0-00731-6.

[16] Kim DH, Paik JK. Ultimate limit state-based multi-objective optimum design technology for hull structural scantlings of merchant cargo ships. Ocean Eng 2017;129:318–34. http://dx.doi.org/10.1016/j.oceaneng.2016.11.033.

[17] Hughes O, K. PJ. Ship structural analysis and design. The Society of Naval Architects and Marine Engineers; 2013, https://www.sname.org/ship-structural-analysis-and-design.

[18] Tartt K, Amiri AK, McDonald A, Jaen-Sola P. Structural optimisation of offshore direct-drive wind turbine generators including static and dynamic analyses. J Phys Conf Ser 2021;2018(1):012040. http://dx.doi.org/10.1088/1742-6596/2018/1/012040.

[19] Benson S, Downes J, Dow RS. Load shortening characteristics of marine grade aluminium alloy plates in longitudinal compression. Thin-Walled Struct 2013;70:19–32. http://dx.doi.org/10.1016/j.tws.2013.04.006.

[20] Benson S, Downes J, Dow RS. Overall buckling of lightweight stiffened panels using an adapted orthotropic plate method. Eng Struct 2015;85:107–17. http://dx.doi.org/10.1016/j.engstruct.2014.12.017.

[21] Putra GL, Kitamura M, Takezawa A. Structural optimization of stiffener layout for stiffened plate using hybrid GA. Int J Nav Archit Ocean Eng 2019;11(2):809–18. http://dx.doi.org/10.1016/j.ijnaoe.2019.03.005.

[22] Pedersen PT, Nielsen NJ. Structural optimization of ship structures. In: Computer aided optimal design: structural and mechanical systems. 1987, http://dx.doi.org/10.1007/978-3-642-83051-8_27.

[23] Cui JJ, Wang DY. Application of knowledge-based engineering in ship structural design and optimization. Ocean Eng 2013;72:124–39. http://dx.doi.org/10.1016/j.oceaneng.2013.06.013.

[24] Yu YY, Jin CG, Lin Y, Ji ZS. A practical method for ship structural optimization. In: International offshore and polar engineering conference. 2010, https://www.researchgate.net/publication/290012996_A_practical_method_for_ship_structural_optimization.

[25] Bayatfar A, Amrane A, Rigo P. Towards a ship structural optimisation methodology at early design stage. Int J Eng Res Dev 2013;9:76–90, http://ijerd.com/paper/vol9-issue6/J09067690.pdf.

[26] Liu B, Guedes Soares C. Ultimate strength assessment of ship hull structures subjected to cyclic bending moments. Ocean Eng 2020;215:107685. http://dx.doi.org/10.1016/j.oceaneng.2020.107685.

[27] Paik JK, Thayamballi AK, Kim DH. An analytical method for the ultimate compressive strength and effective plating of stiffened panels. J Construct Steel Res 1999;49(1):43–68. http://dx.doi.org/10.1016/S0143-974X(98)00207-7.

[28] IACS. Longitudinal strength standard for container ships. 2015, https://iacs.org.uk/download/5936.

[29] Paik JK, Thayamballi AK. An empirical formulation for predicting the ultimate compressive strength of stiffened panels. In: International offshore and polar engineering conference. 1997, https://onepetro.org/ISOPEIOPEC/proceedings/ISOPE97/All-ISOPE97/ISOPE-I-97-444/24245.

[30] Liu B, Gao LJ, Ao L, Wu WG. Experimental and numerical analysis of ultimate compressive strength of stiffened panel with openings. Ocean Eng 2021;220:108453. http://dx.doi.org/10.1016/j.oceaneng.2020.108453.

[31] Frieze PA, Martino A, Mirella V, Paik JK. A benchmark study of ISO 18072-2 on the stiffened panel ultimate strength. In: International conference on offshore mechanics and arctic engineering. 2011, http://dx.doi.org/10.1115/OMAE2011-50152.

[32] Xu MC, Song ZJ, Zhang BW, Pan J. Empirical formula for predicting ultimate strength of stiffened panel of ship structure under combined longitudinal compression and lateral loads. Ocean Eng 2018;162:161–75. http://dx.doi.org/10.1016/j.oceaneng.2018.05.015.

[33] Benson S, Downes J, Dow RS. An automated finite element methodology for hull girder progressive collapse analysis. In: International marine design conference. 2012, https://eprints.ncl.ac.uk/file_store/production/185952/943B856A-D12E-4019-9868-5EAEFA4FD774.pdf.

[34] Li S, Kim DK, Benson S. The influence of residual stress on the ultimate strength of longitudinally compressed stiffened panels. Ocean Eng 2021;108839. http://dx.doi.org/10.1016/j.oceaneng.2021.108839.

[35] Gannon L, Liu Y, Pegg N, Smith MJ. Nonlinear collapse analysis of stiffened plates considering welding-induced residual stress and distortion. Ships Offshore Struct 2016;11:228–44. http://dx.doi.org/10.1080/17445302.2014.985428.

[36] Li S, Benson S, Dow RS. A timoshenko beam finite element formulation for thin-walled box girder considering inelastic buckling. In: International conference on marine structures. 2021, http://dx.doi.org/10.1201/9781003230373.

[37] Li S, Kim DK. A comparison of numerical methods for damage index based residual ultimate limit state assessment of grounded ship hulls. Thin-Walled Struct 2022;172:108854. http://dx.doi.org/10.1016/j.tws.2021.108854.

[38] Shi GJ, Wang DY, Hu B, Cai SJ. Effect of initial geometric imperfections on dynamic ultimate strength of stiffened plate under axial compression for ship structures. Ocean Eng 2022;256:111448. http://dx.doi.org/10.1016/j.oceaneng.2022.111448.

[39] Gannon L, Liu Y, Pegg N, Smith MJ. Effect of welding-induced residual stress and distortion on ship hull girder ultimate strength. Mar Struct 2012;28:25–49. http://dx.doi.org/10.1016/j.marstruc.2012.03.004.

[40] Ringsberg JW, Darie I, Nahshon K, Shilling G, Vaz MA, Benson S, et al. The ISSC 2022 committee III. 1-Ultimate strength benchmark study on the ultimate limit state analysis of a stiffened plate structure subjected to uniaxial compressive loads. Mar Struct 2021;79:103026. http://dx.doi.org/10.1016/j.marstruc.2021.103026.

[41] Paik J, Amlashi A, Boon B, Branner K, Caridis P, Das P, et al. Committee III.1 ultimate strength. In: Fricke W, Bronsart R, editors. International ship and offshore structures congress. 2012, p. 285–363, http://www.issc2022.org/wp-content/uploads/issc2012-vol1-com-III.1.pdf.

[42] Li S, Coraddu A, Oneto L. Computationally aware estimation of ultimate strength reduction of stiffened panels caused by welding residual stress: From finite element to data-driven methods. Eng Struct 2022;264:114423. http://dx.doi.org/10.1016/j.engstruct.2022.114423.

[43] Shalev-Shwartz S, Ben-David S. Understanding machine learning: from theory to algorithms. Cambridge University Press; 2014, http://dx.doi.org/10.1017/CBO9781107298019.

[44] Goodfellow I, Bengio Y, Courville A, Bengio Y. Deep learning. MIT press Cambridge; 2016, http://www.deeplearningbook.org.

[45] Waltz RA, Morales JL, Nocedal J, Orban D. An interior algorithm for nonlinear optimization that combines line search and trust region steps. Math Program 2006;107(3):391–408. http://dx.doi.org/10.1007/s10107-004-0560-5.

[46] Powell MJD. The convergence of variable metric methods for nonlinearly constrained optimization calculations. In: Nonlinear programming, vol. 3. 1978, http://dx.doi.org/10.1016/B978-0-12-468660-1.50007-4.

[47] Kramer O. Genetic algorithm essentials. Springer; 2017, http://dx.doi.org/10.1007/978-3-319-52156-5.

[48] Kennedy J, Eberhart R. Particle swarm optimization. In: IEEE international joint conference on neural networks. 1995, http://dx.doi.org/10.1109/ICNN.1995.488968.

[49] Doan VT, Liu B, Garbatov Y, Wu WG, Guedes Soares C. Strength assessment of aluminium and steel stiffened panels with openings on longitudinal girders. Ocean Eng 2020;200:107047. http://dx.doi.org/10.1016/j.oceaneng.2020.107047.

[50] Tanaka S, Yanagihara D, Yasuoka A, Harada M, Okazawa S, Fujikubo M, et al. Evaluation of ultimate strength of stiffened panels under longitudinal thrust. Mar Struct 2014;36:21–50. http://dx.doi.org/10.1016/j.marstruc.2013.11.002.

[51] Shanmugam NE, Q. ZD, Choo YS, Arockiaswamy M. Experimental studies on stiffened plates under in-plane load and lateral pressure. Thin-Walled Struct 2014;80:22–31. http://dx.doi.org/10.1016/j.tws.2014.02.026.

[52] Smith CS, Davidson PC, Chapman JC. Strength and stiffness of ships' plating under in-plane compression and tension. Trans RINA 1987;130:277–93, https://www.rina.org.uk/RINA_Transactions.html.

[53] Smith CS, Anderson N. Strength of stiffened plating under combined compression and lateral pressure. Trans RINA 1991;134:131–47, https://www.rina.org.uk/RINA_Transactions.html.

[54] Benson S, Downes J, Dow RS. Ultimate strength characteristics of aluminium plates for high-speed vessels. Ships Offshore Struct 2011;6:67–80. http://dx.doi.org/10.1080/17445302.2010.529696.

[55] Gordo J. Effect of initial imperfections on the strength of restrained plates. J Offshore Mech Arct Eng 2015;137:051401. http://dx.doi.org/10.1115/1.4030927.

[56] Akpan UO, Koko TS, Ayyub BM, Dunbar T. Reliability-based optimal design of steel box structures. I: Theory. ASCE-ASME J Risk Uncertain Eng Syst A 2015;1(3):04015009. http://dx.doi.org/10.1061/AJRUA6.0000829.

[57] Akpan UO, Koko TS, Ayyub BM, Dunbar T. Reliability-based optimal design of steel box structures. II: Ship structure applications. ASCE-ASME J Risk Uncertain Eng Syst A 2015;1:04015010. http://dx.doi.org/10.1061/AJRUA6.0000830.

[58] Tushaj E, Lako N. A review of structural size optimization techniques applied in the engineering design. Int J Sci Eng Res 2017;8:706–14, https://www.ijser.org/.

[59] Perez RE, Behdinan K. Particle swarm approach for structural design optimization. Comput Struct 2007;85(19):1579–88. http://dx.doi.org/10.1016/j.compstruc.2006.10.013.

[60] Fadaee MJ, Grierson DE. Design optimization of 3D reinforced concrete structures having shear walls. Eng Comput 1998;14:139–45. http://dx.doi.org/10.1007/BF01213587.

[61] Gentils T, Wang L, Kolios A. Integrated structural optimisation of offshore wind turbine support structures based on finite element analysis and genetic algorithm. Appl Energy 2017;199:187–204. http://dx.doi.org/10.1016/j.apenergy.2017.05.009.

[62] Fadel Miguel LF, Lopez RH, Torii AJ, Beck AT. Reliability-based optimization of multiple folded pendulum TMDs through efficient global optimization. Eng Struct 2022;266:114524.

[63] Cao HY, Qian XD, Chen ZJ, Zhu HP. Layout and size optimization of suspension bridges based on coupled modelling approach and enhanced particle swarm optimization. Eng Struct 2017;146:170–83.

[64] Benzo PG, Pereira JM, Sena-Cruz J. Optimization of steel web core sandwich panel with genetic algorithm. Eng Struct 2022;253:113805.

[65] Franchini A, Sebastian W, D'Ayala D. Surrogate-based fragility analysis and probabilistic optimisation of cable-stayed bridges subject to seismic loads. Eng Struct 2022;256:113949.

[66] Picchi Scardaoni M, Izzi MI, Montemurro M, Panettieri E, Cipolla V, Binante V. Multi-scale deterministic optimisation of blended composite structures: case study of a box-wing. Thin-Walled Struct 2022;170:108521.

[67] Li QQ, Wu LJ, Tao Chen T, Li E, Hu L, Wang F, et al. Multi–objective optimization design of B–pillar and rocker sub–systems of battery electric vehicle. Struct Multidiscip Optim 2021;64:3999–4023. http://dx.doi.org/10.1007/s00158-021-03073-0.

[68] Scott S, Greaves P, Weaver PM, Pirrera A, Macquart T. Efficient structural optimisation of a 20 MW wind turbine blade. J Phys Conf Ser 2020;1618:042025. http://dx.doi.org/10.1088/1742-6596/1618/4/042025.

[69] Sekulski Z. Ship hull structural multiobjective optimization by evolutionary algorithm. J Ship Res 2014;58(2):1–25. http://dx.doi.org/10.5957/jsr.2014.58.2.45.

[70] Du L, Pinto GO, Hefazi H, Sahoo P. Trimaran structural weight optimization based on classification rules. J Ship Prod Des 2018;00:1–10. http://dx.doi.org/10.5957/JSPD.170033.

[71] Hughes O, Ma M, Paik JK. Application of vector evaluated genetic algorithm (VEGA) in ultimate limit state based ship structural design. In: International conference on ocean, offshore and arctic engineering. 2014, http://dx.doi.org/10.1115/OMAE2014-23379.

[72] Ma M, Hughes O, McNatt T. Ultimate limit state based ship structural design using multi-objective discrete particle swarm optimization. In: International conference on ocean, offshore and arctic engineering. 2015, http://dx.doi.org/10.1115/OMAE2015-41456.

[73] ALPS/HULL. A computer program for progressive collapse analysis of ship hulls. 2016, https://www.maestromarine.com/maestro-base-module/apps-hull/.

[74] Ehlers S. A procedure to optimize ship side structures for crashworthiness. Proc Inst Mech Eng M 2010;224(1):1–11. http://dx.doi.org/10.1243/14750902JEME179.

[75] Lou H, Gao B, Jin F, Wan Y, Wang Y. Shear wall layout optimization strategy for high-rise buildings based on conceptual design and data-driven tabu search. Comput Struct 2021;250:106546. http://dx.doi.org/10.1016/j.compstruc.2021.106546.

[76] Huang H, Xue C, Zhang W, Guo M. Torsion design of CFRP-CFST columns using a data-driven optimization approach. Eng Struct 2022;251:113479. http://dx.doi.org/10.1016/j.engstruct.2021.113479.

[77] Singh K, Kapania RK. Accelerated optimization of curvilinearly stiffened panels using deep learning. Thin-Walled Struct 2021;161:107418. http://dx.doi.org/10.1016/j.tws.2020.107418.

[78] Hao P, Liu D, Zhang K, Yuan Y, Wang B, Li G, et al. Intelligent layout design of curvilinearly stiffened panels via deep learning-based method. Mater Des 2021;197:109180. http://dx.doi.org/10.1016/j.matdes.2020.109180.

[79] Cui H, Turan O, Sayer P. Learning-based ship design optimization approach. Comput Aided Des 2012;44(3):186–95. http://dx.doi.org/10.1016/j.cad.2011.06.011.

[80] Fang C, Ping YW, Gao YG, Zheng Y, Chen YY. Machine learning-aided multi-objective optimization of structures with hybrid braces – Framework and case study. Eng Struct 2022;269:114808.

[81] Guo BC, Lin XS, Wu YF, Zhang LH. Machine learning-driven evaluation and optimisation of compression yielded FRP-reinforced concrete beam with t section. Eng Struct 2023;275:115240.

[82] Faulkner D, Adamchak JC, Snyder GJ, Vetter MF. Synthesis of welded grillages to withstand compression and normal loads. Comput Struct 1973;3(2):221–46. http://dx.doi.org/10.1016/0045-7949(73)90015-1.

[83] Kumakura Y, Sasajima H. A consideration of life cycle cost of a ship. In: Practical design of ships and other floating structures. 2001, http://dx.doi.org/10.1016/B978-008043950-1/50004-1.

[84] Paik JK, Kim BJ, Seo JK. Methods for ultimate limit state assessment of ships and ship-shaped offshore structures: Part II stiffened panels. Ocean Eng 2008;35(2):271–80. http://dx.doi.org/10.1016/j.oceaneng.2007.08.007.

[85] Chalmers DW. Design of ships' structures. UK Ministry of Defence; 1993.

[86] Emmerich M, Deutz AH. A tutorial on multiobjective optimization: Fundamentals and evolutionary methods. Nat Comput 2018;17(3):585–609. http://dx.doi.org/10.1007/s11047-018-9685-y.

[87] Kochenderfer MJ, Wheeler TA. Algorithms for decision making. Mit Press; 2022, https://algorithmsbook.com/.

[88] Wolpert DH, Macready WG. No free lunch theorems for optimization. IEEE Trans Evol Comput 1997;1(1):67–82. http://dx.doi.org/10.1109/4235.585893.

[89] Martí R. Multi-start methods. In: Handbook of metaheuristics. 2003, http://dx.doi.org/10.1007/978-1-4419-1665-5.

[90] Naser MZ, Alavi AH. Error metrics and performance fitness indicators for artificial intelligence and machine learning in engineering and sciences. Archit Struct Construct 2021;1–19. http://dx.doi.org/10.1007/s44150-021-00015-8.

[91] Sainani KL. The value of scatter plots. PM&R 2016;8(12):1213–7. http://dx.doi.org/10.1016/j.pmrj.2016.10.018.

[92] Paik JK, Kim DK, Park DH, Kim HB, Mansour AE, Caldwell JB. Modified Paik–Mansour formula for ultimate strength calculations of ship hulls. Ships Offshore Struct 2013;8(3–4):245–60. http://dx.doi.org/10.1080/17445302.2012.676247.

[93] Frankland JM. The strength of ship plating under edge compression. 1940, https://dome.mit.edu/handle/1721.3/48082.